



## COMPUTER AIDED DESIGN AND NUMERICAL ANALYSIS OF INVOLUTE SPUR GEAR – A NOVEL STUDY BY FEA

Simon Christopher A

Department of Mechanical Engineering, V V College of Engineering, Tisaiyanvillai,- 627 657, Tamilnadu, India.

### ABSTRACT

Gears are widely used in transmission system which undergoes cyclic loads in service. Maximum load transmitted by the gear has been an important factor in designing of a gear. The maximum stress induced on the gear tooth when it meshes with other gear should be less than its capability so that its life will be lasting. It is necessary to understand the deformations and stresses induced in the components are within the desirable limit. So it is necessary to analyze the load acting on the tooth while transmission and the corresponding induced stress on the gear tooth. Based on the above said analysis the induced stress is predicted on the tooth. The force and stress analysis is made to justify the result by analytically and using FEA tools. A spur gear profile was created MATLAB programming. A CAD model was created using SolidWorks software. FEA analysis was performed using ANSYS. The present study elucidates the mechanical and bending behavior of spur gear tooth. It can serve as valuable basis to enhance more accurate models, and obtaining all numerical parameters needed for elaboration of the system.

**Keywords:** *Involute Gear, MAT Lab and Numerical Analysis.*

### 1. Introduction

A number of researchers have worked on gear tooth failure and used experimental, analytical and numerical techniques to determine the stresses in the gear tooth. Most commonly used experimental techniques include photo elastic and strain gages, and finite element method was the mostly used numerical technique.

Photo elastic technique was widely used for many years. Baud and Timoshenko [1] introduced the photo elastic technique to examine the stress concentration effect at the gear tooth fillets. Sopwith and Heywood [2] used photo elastic technique to develop a fillet stress formula that accounted for some pressure angle unbalance. Kelly and Pederson [3] improved this formula by employing more realistic tooth shapes in their photo elastic models.

Gear tooth damage can be caused by a variety of factors including inadequate lubrication, inappropriate operating conditions or specifications, material insufficiencies, and manufacturing or installation problems. Effective lubrication of gear systems is of critical importance because it prevents direct tooth contact, reduces friction and vibration levels, removes heat generated in the mesh, and protects the gears from corrosion. When the tooth surfaces are subjected to excessive stress conditions, tooth surface failure may occur. This can cause removal and/or plastic deformation of the contacting tooth surfaces [4–6]. In some cases, surface fatigue cracks occur in plastically

deformed regions under excessive contact stress, and these can also be caused by scuffing or wear failure [7,8].

In order to improve load carrying capacity of the gears Litvin F. L. Et al. [9] and Tsai M. et al. [10] focused there research work to design the stronger tooth profiles. Hoffmann G. et al. [11] developed advanced material for high load gear applications. Townsend D. P et al. [12], Legge G. [13], and Herring D. H. [14], proposed improved methods on heat treatment.

In the earlier work, the gear tooth profile has not been modelled accurately. In this work the accurate spur gear tooth profile was generated by using MAT Lab programming. The Computer Aided Design (CAD) model of the gear was created using Solid Works. Finite Element Analysis (FEA) of spur gear was performed using ANSYS. The load carrying capacity of numerical method was compared with the analytical results.

### 2. Spur Gear Design

This analysis work concentrates on the reliability and durability of the gear so a random input data is assumed to design the spur gear. Based on the given input data the required gear is designed. Also the involute profile is generated as discussed earlier.

Input Data:

Power : 20 kW

Pinion speed : 1400 rpm

\*Corresponding Author - E- mail: [tsysimon@gmail.com](mailto:tsysimon@gmail.com)

Wheel speed: 350 rpm

### 2.1 Spur Gear Design Output from Matlab

Based on the above mentioned input data, a MatLab program was developed. Using the same program, a spur gear design calculation was performed.

### 2.2 Spur Gear Tooth Profile Output from Matlab

The involute profile was made simple by creating MatLab program which has been presented in Appendix. The profile obtained by the developed programme is presented in Fig.1. The data used for the creation of the curve has been used for the generation of the CAD model and later for numerical analysis.

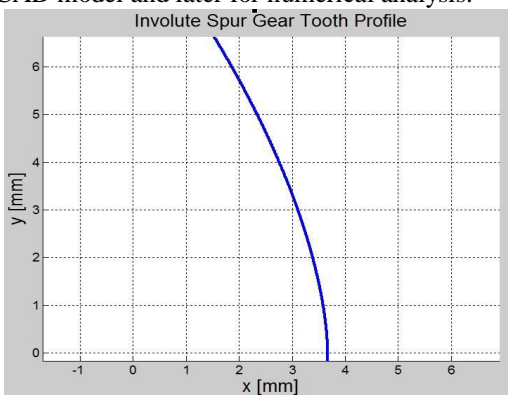


Fig. 1. Required Spur gear Tooth Profile

### 2.3 Spur Gear Modelling in CAD

The coordinated obtained through Matlab coding has been used for the creation of CAD model with the actual dimensions. For modelling the gear Solid Works 2008 was used.

### 2.4 Procedure to Create Spur Gear in CAD

#### STEP-1: Importing coordinates into CAD tool.

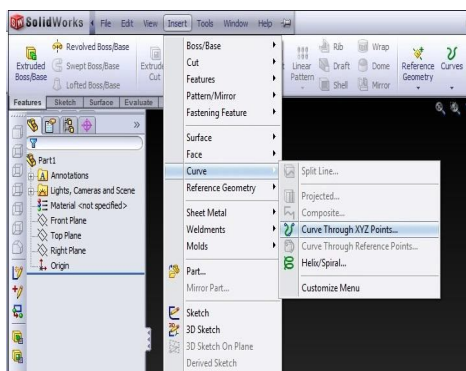


Fig. 2. Importing Coordinates into CAD Tool

The result obtained from the Matlab program was stored in a text file. The text file contains the X,Y,Z coordinates of involute profile. The text document was imported into Solid Works by using “curve through xyz point” option.

#### STEP-2: Generating in-volute profile in CAD tool

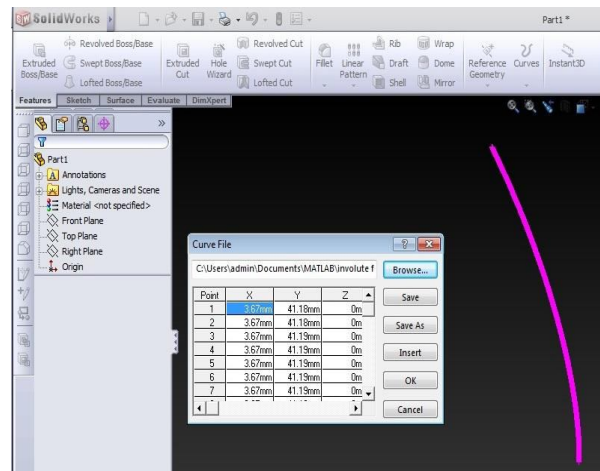


Fig 3. Generating Involute Profile in CAD Tool

Once the coordinates are imported the data table has been filled with the xyz points and the profile is generated.

#### Profiles in Matlab and CAD:

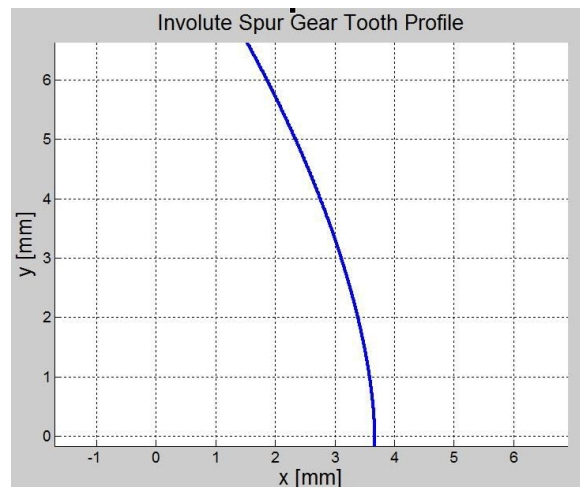
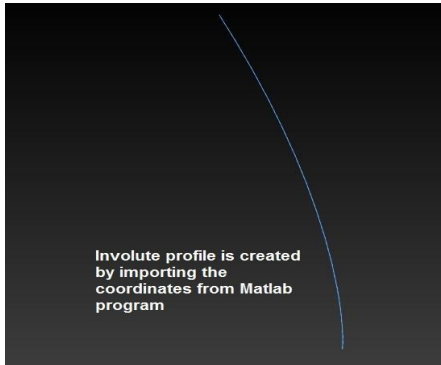
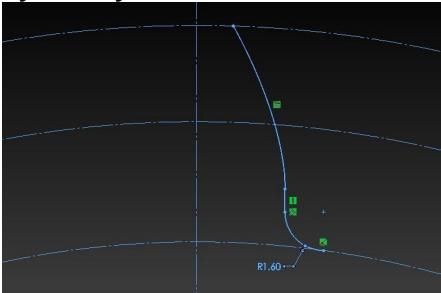


Fig. 4. Involute Profile Generated in MatLab



**Fig 5. Involute Profile Created in CAD**

**STEP-3: Creation of root circle, tip circle, pitch circle, symmetry axis and root fillet.**



**Fig. 6. Creating Root Circle, Tip circle, Pitch Circle, Symmetry Axis and Root Fillet**

Since the working depth of profile was created from calculation, clearance portion was created in CAD. The required reference circles were created in this step.

**STEP-4: Symmetry profile creation**

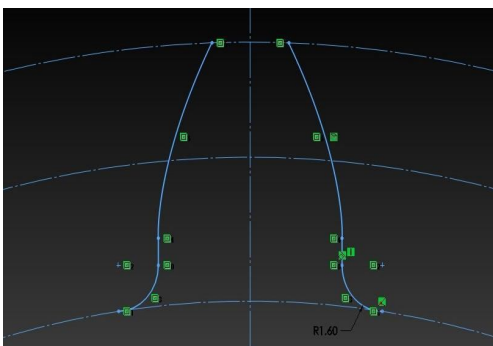


**Fig. 7. Symmetry Profile Creation**

In this step the imported profile is mirrored so as to create an involute spur gear teeth profile.

**STEP-5: Creating required no of teeth**

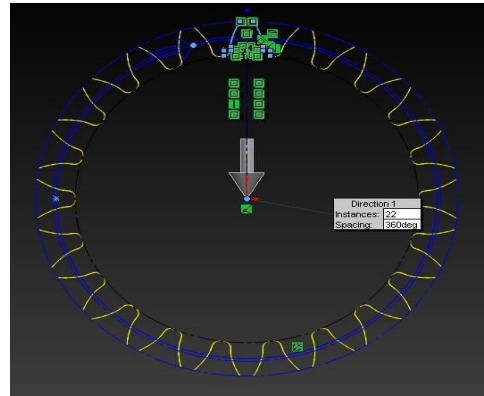


**Fig 8. Creating Required Number of Teeth**

After creating a full teeth profile, it is used to generate required 22 no of spur gear teeth profile.

**STEP-6: Creating 3D CAD model of spur gear**

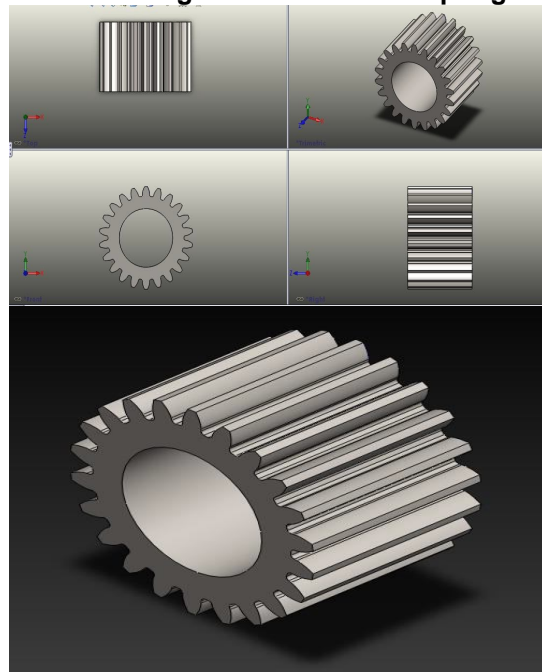


**Fig. 9. Creating 3D CAD Model of Spur Gear**

After creating the circular array of 2D involute tooth, it was used to create 3D CAD model.

**2.5 Drafting**

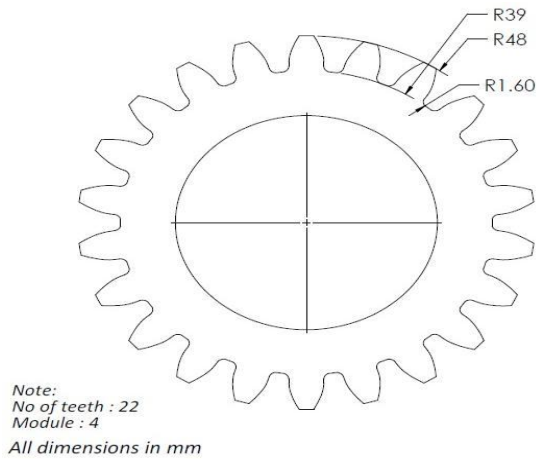


Fig. 10. Drafting

As calculated earlier the required spur gear is modelled in CAD with 22 involute teeth, tooth circle dia of 96 mm, root circle dia of 78 mm, width of 66 mm. This CAD model can be used in FEA analysis.

### 3. Force Analysis of Spur Gear

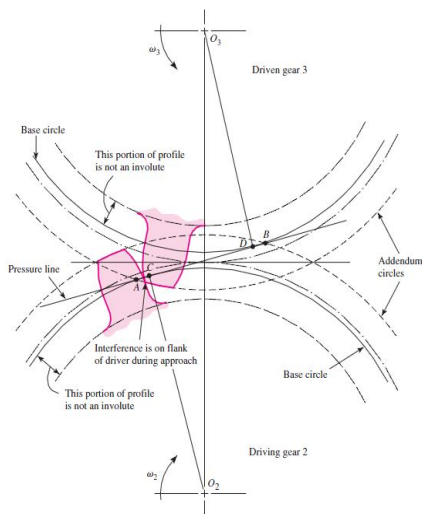


Fig. 11. Force Analysis of Spur Gear

Before beginning the force analysis of gear trains, let us agree on the notation to be used. Beginning with the numeral 1 for the frame of the machine, we shall designate the input gear as gear 2, and then number the gears successively 3, 4, etc., until we arrive at the

last gear in the train. Next, there may be several shafts involved, and usually one or two gears are mounted on each shaft as well as other elements.

We shall designate the shafts, using lowercase letters of the alphabet, a, b, c, etc. With this notation we can now speak of the force exerted by gear 2 against gear 3 as  $F_{23}$ . The force of gear 2 against a shaft a is  $F_{2a}$ . We can also write  $F_{a2}$  to mean the force of a shaft a, against gear 2. Unfortunately, it is also necessary to use superscripts to indicate directions. The coordinate directions will usually be indicated by the x, y, and z coordinates, and the radial and tangential directions by superscripts r and t. With this notation,  $F_{t43}$  is the tangential component of the force of gear 4 acting against gear 3.

Fig 11, shows a pinion mounted on shaft a rotating clockwise at  $n_2$  rev/min and driving a gear on shaft b at  $n_3$  rev/min. The reactions between the mating teeth occur along the pressure line. In Fig 11, the pinion has been separated from the gear and the shaft, and their effects have been replaced by forces.  $F_{a2}$  and  $T_{a2}$  are the force and torque, respectively, exerted by shaft a, against pinion 2.  $F_{32}$  is the force exerted by gear 3 against the pinion.

Using a similar approach, we obtain the free-body diagram of the gear shown in Fig 12. In Fig 13, the free-body diagram of the pinion has been redrawn and the forces have been resolved into tangential and radial components.

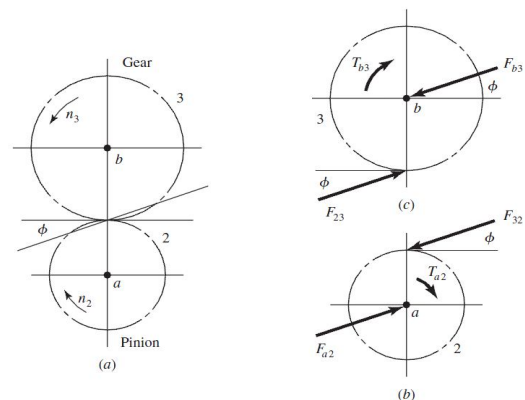


Fig 12. Free-Body Diagram of the Gear

We now define,

$$W_t = Ft_{32} \tag{1}$$

This tangential load is really the useful component, because the radial component  $F_{r32}$  serves no useful purpose. It does not transmit power. The applied torque and the transmitted load are seen to be related by the equation.

$$T = (d/2) W_t \tag{2}$$

Where we have used  $T = T_{a2}$  and  $d = d_2$  to obtain a general relation.

The power  $H$  transmitted through a rotating gear can be obtained from the standard relationship of the product of torque  $T$  and angular velocity  $\omega$ .

$$H = T\omega = (Wt \, d/2) \, \omega \quad (3)$$

While any units can be used in this equation (3), the units of the resulting power will obviously be dependent on the units of the other parameters. It will often be desirable to work with the power in either horsepower or kilowatts, and appropriate conversion factors should be used.

Since meshed gears are reasonably efficient, with losses of less than 2 percent, the power is generally treated as constant through the mesh. Consequently, with a pair of meshed gears, Eq. for  $H$ , will give the same power regardless of which gear is used for  $d$  and  $\omega$ .

Gear data is often tabulated using pitch-line velocity, which is the linear velocity of a point on the gear at the radius of the pitch circle; thus  $V = (d/2) \, \omega$ . Converting this to customary units gives

$$V = \pi d n / 12 \quad (4)$$

Where,  $V$  - pitch-line velocity, ft/min  
 $d$  - gear diameter, in  
 $n$  - gear speed, rev/min

Many gear design problems will specify the power and speed, so it is convenient to solve Eqn (3),  $H$  for  $Wt$ . With the pitch-line velocity and appropriate conversion factors incorporated, Eqn (3),  $H$  can be rearranged and expressed in customary units as

$$Wt = 33000 \cdot (H/V) \quad (5)$$

Where,  
 $Wt$  - transmitted load, lbf  
 $H$  - power, hp  
 $V$  - pitch-line velocity, ft/min  
 The corresponding equation (5) in SI

is

$$Wt = 60000 \cdot H / (\pi d n)$$

Where,  
 $Wt$  = transmitted load, kN  
 $H$  = power, kW  
 $d$  = gear diameter, mm  
 $n$  = speed, rev/min

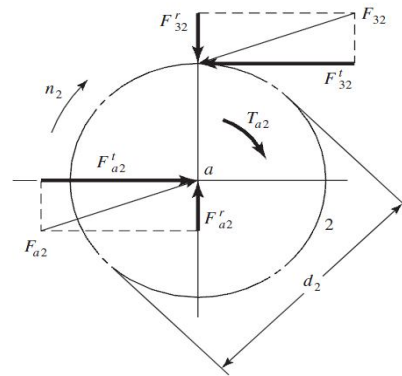


Fig 13. Resolved Forces

As mentioned above transmitted tangential load has been

$$\begin{aligned} Wt &= 60000 \cdot H / (\pi d n) \\ &= 60000 \cdot 20 / (\pi \cdot 88 \cdot 1400) \\ &= 1.2 \cdot 106 / 387044.21 \\ Wt &= 3.1 \text{ kN} \end{aligned}$$

#### 4. The Lewis Bending Equation

Wilfred Lewis introduced an equation for estimating the bending stress in gear teeth in which the tooth form entered into the formulation. The equation, announced in 1892, still remains the basis for most gear design today. To derive the basic Lewis equation, refer to Fig 14 (a), which shows a cantilever of cross-sectional dimensions  $F$  and  $t$ , having a length  $l$  and a load  $Wt$ , uniformly distributed across the face width  $F$ . The section modulus  $I/c$  is  $Ft^2/6$ , and therefore the bending stress is,

$$\begin{aligned} \sigma &= M / (I/c) \\ &= 6Wt \, l / (Ft^2) \end{aligned} \quad (6)$$

Gear designers denote the components of gear-tooth forces as  $Wt$ ,  $Wr$ ,  $Wa$  or  $Wt$ ,  $Wr$ ,  $Wa$  interchangeably. The latter notation leaves room for post-subscripts essential to free body diagrams. For instance, for gears 2 and 3 in mesh,  $Wt_{23}$  is the transmitted force of body 2 on body 3, and  $Wt_{32}$  is the transmitted force of body 3 on body 2.

When working with double-or triple-reduction speed reducers, this notation is compact and essential to clear thinking. Since gear-force components rarely take exponents, this causes no complication. Pythagorean combinations, if necessary, can be treated with parentheses or avoided by expressing the relations trigonometrically.

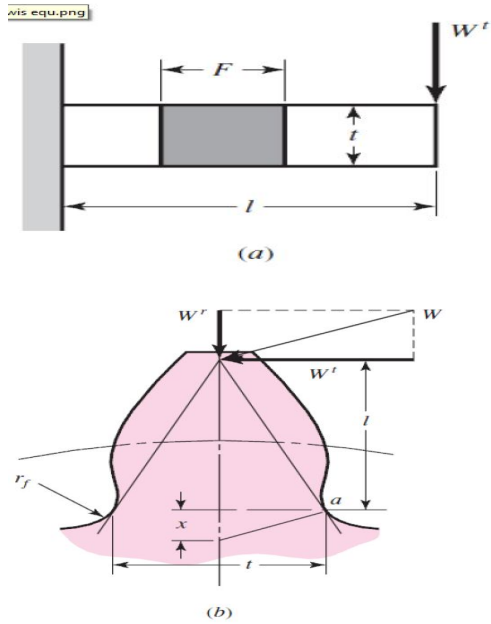


Fig. 14. (a) & (b) The Lewis Bending Equation

Referring now to Fig 14 (b), we assume that the maximum stress in a gear tooth occurs at point *a*. By similar triangles, you can write

$$\frac{t/2}{x} = \frac{l}{t/2} \quad \text{or} \quad x = \frac{t^2}{4l} \quad (7)$$

$$\sigma = \frac{6W^t l}{F t^2} = \frac{W^t}{F} \frac{1}{t^2/6l} = \frac{W^t}{F} \frac{1}{t^2/4l} \frac{4}{6} \quad (8)$$

If we now substitute the value of *x* and multiply the numerator and denominator by the circular pitch *p*, we find,

$$\sigma = \frac{W^t p}{F \left(\frac{2}{3}\right) x p} \quad (9)$$

Letting  $y = 2x/3p$ , we have

$$\sigma = \frac{W^t}{F p y} \quad (10)$$

This completes the development of the original Lewis equation. The factor *y* is called the Lewis form factor, and it may be obtained by a graphical layout of the gear tooth or by digital computation.

In using this equation (10), most engineers prefer to employ the diametral pitch in determining the stresses. This is done by substituting,

$$P = \pi/p \quad \text{and} \quad Y = \pi y$$

This gives,

$$\sigma = \frac{W^t P}{F Y} \quad (11)$$

Where, The use of this equation for

$$Y = \frac{2xP}{3} \quad (12)$$

*Y* means that only the bending of the tooth is considered and that the compression due to the radial component of the force is neglected. Values of *Y* obtained from this equation (12) are tabulated in table

Table 4: The Lewis Form Factor for Number of Teeth

No of Teeth	Lewis form factor, y	No of Teeth	Lewis form factor, y
12	0.245	28	0.353
13	0.261	30	0.359
14	0.277	34	0.371
15	0.290	38	0.384
16	0.296	43	0.397
17	0.303	50	0.409
18	0.309	60	0.422
19	0.314	75	0.435
20	0.322	100	0.447
21	0.328	150	0.460
22	0.331	300	0.472
24	0.337	400	0.480
26	0.346	Rack	0.485

The use of Equation (12) also implies that the teeth do not share the load and that the greatest force is exerted at the tip of the tooth. But we have already learned that the contact ratio should be somewhat greater than unity, say about 1.5, to achieve a quality gear set. If, in fact, the gears are cut with sufficient accuracy, the tip-load condition is not the worst, because another pair of teeth will be in contact when this condition occurs.

Examination of run-in teeth will show that the heaviest loads occur near the middle of the tooth. Therefore the maximum stress probably occurs while a



single pair of teeth is carrying the full load, at a point where another pair of teeth is just on the verge of coming into contact.

Also from the design calculation of required gear and pinion component the bending stress is obtained as 44.8441 MPa for pinion.

## 5. Bending Stress Analysis by Numerical Method

### 5.1 FEM modelling

The 3D CAD model was imported as IGES format into Ansys Workbench environment. In order to reduce the computation time the 3D spur gear model is reduced into 3 teeth segment using Ansys Design Modeller. Since it has equal cross sections the mid plane of reduced model was extracted for further analysis, it will act as planar model.

Element Order	2D Solid	3D Solid	3D Shell	Line Elements
Linear	PLANE42 PLANE182	SOLID45 SOLID185	SHELL63 SHELL181	BEAM3/44 BEAM188
	PLANE82/183 PLANE2	SOLID95/186 SOLID92/187	SHELL93	BEAM189

Fig. 15. Types of Linear and Quadratic Elements

Ansys Mesh Modeller uses Shell181 which is the newest element and replacing PLANE42 in the workbench environment. It has the capability to analyze thin to finite strain models. It will provide same results as PLANE42.

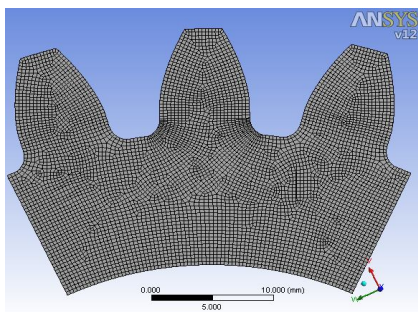


Fig 16. Three Teeth Segment using Ansys Design Modeller

Global and local element controls are set in the model. Initially element is set to 0.3mm global size and the root fillet is refined with 0.1mm element size.

The model then constrained as cantilever. And the radial load was neglected and the tangential load is calculated and applied to its central teeth. The linear static analysis is performed with initial mesh size and then adaptive convergence is added for its stress refinement with 5% of convergence. Due to limitations in the hardware capability the convergence criteria is set to 5%. The final refinement produces no of elements and change in accuracy as follow,

The result is obtained as follow, the contour plots are obtained for the reduced FEM model.

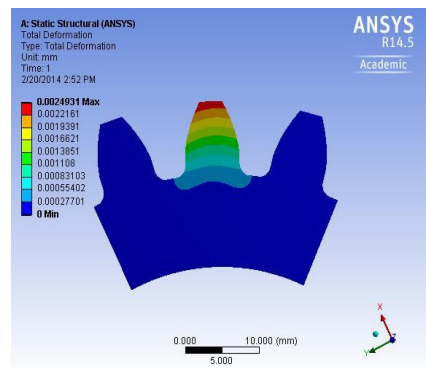


Fig. 17. Contour Plot for Total Deformation

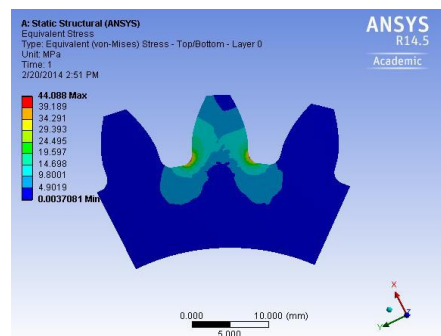
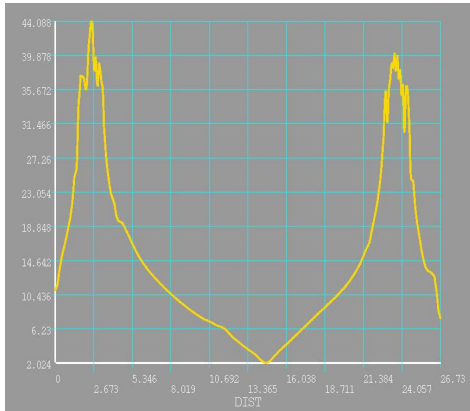


Fig. 18. Contour Plot for Equivalent Stress

The results are compared with calculated values as follow, the stress distribution on the central teeth was extracted and plotted graphically as follows,



**Fig. 19. Stress Distribution**

Where,

X Axis - Selected nodes around the gear teeth profile

Y Axis - Stress distribution on the central teeth

The plot shows the stress distributed on the involute profile during loading. The peak values show the stress induced at the root of spur tooth. It is observed that higher stress values are observed at the tensile side of root and lower stress are observed at the compressive side of root.

## 6. Conclusions

The present work was aimed to study the spur gear design, involute profile calculation and its integrity analysis.

For the chosen input load, a spur gear was designed using MATLAB programming, calculation of involute gear tooth profile was plotted using MATLAB programming. Using these calculated data spur gear design data and involute profile data were imported into Solidworks software. The Computer Aided Design (CAD) model was created in SolidWorks software for further analysis. A symmetric model was used for the analysis. Finite Element Analysis (FEA) of spur gear was performed using. The bending stress calculation using Lewis equation and FEA was validated. The result shows noticeable agreement.

The approach demonstrated in this study may be used for any kind of gears / components through which optimal attributes can be arrived.

## References

1. Timoshenko S and Baud R V (1926), "Strength of Gear Teeth", *Mechanical Engineering*, Vol. 48 (11), 1108.
2. Sopwith D G and Heywood R B (1948), "Loads and Stresses in Screw Threads and Projections", *Applied Mechanics Division of the Institution of Mechanical Engineers*, Vol.159.
3. Kelly B W and Pedersen R (1957), "The Beam Strength of Modern Gear Tooth Design", *SAE Earthmoving Industry Conference, Peoria, IL*.
4. Merit H E (1971), "Gear Engineering", *England: Pitman*.
5. Balmforth N and Watson H J (1965), "A Practical Look at Gear-Tooth Damage, *Proceedings of the Institution of Mechanical Engineers*, Vol. 179 (3D), 201-20.
6. Drago R J (1988), "Fundamentals of Gear Design. USA: Butterworth.
7. Johnson K L (1989), "The Strength of Surfaces in Rolling Contact, *Proceedings of the Institution of Mechanical Engineers*, Vol. 203, 151-63.
8. Coleman W (1968), "Bevel Hypoid Gear Surface Durability: Pitting and Scuffing, *Proceedings of the Institution of Mechanical Engineers*, Vol. 182, 191-204.
9. Litwin F L Qiming L and Kapelvich A L (2000), "Asymmetric Modified Spur Gear Drives: Reduction of Noise, Localization of Contact, Simulation of Meshing and Stress Analysis, *Computer Methods in App, Mechanics and Eng*, Vol. 188, 363-390.
10. Tsai M and Tsai Y (1998), "Design of High Contact Ratio Spur Gears Using Quadratic Parametric Tooth profiles, *Mechanism and Machine Theory*, Vol. 33, 551-542.
11. Hoffman G et al., (1999), "Testing P/M Materials for High Loading Gear Application, *International Journal of Powder Metallurgy*, Vol. 35, 35-44.
12. Townsed D P and Bambeger E N (1991), "Surface Fatigue Life of Carburized and Hardened M50NiL and AISI 9310 Spur Gears and Rolling Contact Test Bars, *Journal of Propulsion and Power*, Vol. 7.
13. Legge G (1988), "Plasma Carburizing-Facility Design and Operating Data", *Industrial Heating*, 26-30.
14. Herring D H (1987), "Why Vacuum Carburizing Is Effective for Today and Tomorrow: II, *Industrial Heating*, 22-26.